International Journal of Thermophysics, Vol. 14, No. 5, 1993

Sensitivities of Measurement Methods for the Thermal Radiative Properties and Optical Constants of Metals in the Spectral Range 0.4 to 10 μm

M. A. Havstad[1] **and S. A. Self**[2]

Received January 25, 1993

The sensitivities to measurement errors and potential effectiveness of six methods (involving reflection, emission, and ellipsometry) for determining the optical constants (index of refraction n and extinction coefficient k) of isotropic conductors are compared. The methods treated are generally regarded as most promising for use with high-temperature solid and liquid metals with smooth surfaces of high purity. For each method, contours of constant measured variable are plotted vs n and k. By analysis of the spacing and angle of intersection of these contours, we show that only methods based on measuring both amplitude attenuation and phase shift on reflection can yield n and k, and thus the spectral and directional emissivity, reflectivity, and absorptivity, with reasonable precision over the spectral range 0.4 to 10 μm. Methods based only on amplitude attenuation on reflection, or on the angular dependence of emission, are poorly suited to ranges of n and k that are typical of the infrared. The method of Beattie and Conn retains the ability to determine both optical constants to 10 μm.

KEY WORDS: ellipsometry; extinction coefficient; index of refraction; optical properties; thermal radiative properties.

1. INTRODUCTION

The optical constants of an isotropic material are given by the real and imaginary components n and k of the complex index of refraction $N = n - ik$, where n is the index of refraction and k is the extinction coefficient. These quantities are of interest in the study of the electronic

[1] Lawrence Livermore National Laboratory, P.O. Box 808, Livermore, California 94550, U.S.A.

[2] Department of Mechanical Engineering, Stanford University, Palo Alto, California, U.S.A.

0195-928X/93/0900-1077$07.00/0 © 1993 Plenum Publishing Corporation

structure of materials and in a wide range of technologies. Accurate values of the optical constants of metals, which are significant functions of wavelength, are of particular interest in laser welding, metal refining, electron-beam processing, vacuum-arc remelting, and laser isotope separation because of their influence on heat transfer in such applications. The optical constants determine the reflective, emissive, and absorptive properties (collectively called the thermal radiative properties) of the high-temperature solid and liquid metal surfaces in these technologies. For processes with temperatures from 900 to 1600 K and higher, the optical constants are required over an extended spectral range, 0.4 to 10 μm, in order to specify material properties over all wavelengths in which appreciable radiative energy is present (as given by the Planck function).

Measurement methods for the optical constants in this spectral range are numerous [1–6]. Ellipsometric and polarimetric methods are common but complex. Reflection measurements at multiple angles of incidence are used in the visible, but rarely in the IR, where reflectivities are commonly near 1. Emission measurements at multiple angles of incidence require samples at elevated temperatures, often above 1100 K. Kramers–Kronig methods require assumptions about the sample's optical properties outside the range of measurement. Transmission methods are not practical with metals because sufficiently thin samples are difficult to produce, and such samples may not be representative of the bulk material.

The sensitivities of these methods to measurement errors vary greatly, particularly in the IR, so that they must be compared over the entire parameter space of interest to identify the most practical approach to obtaining the optical constants. This paper compares the six most practical reflection, emission, and ellipsometric methods to assess their suitability for determining the optical constants of clean metallic surfaces between 0.4 and 10 μm. Kramers–Kronig methods are omitted because they cannot be used to obtain n and k from data at a single wavelength. The sensitivities of the methods are determined by examining plots of measured quantities in the n, k plane.

Spectral range is critical to the choice of measurement method because of the variation of n and k with wavelength. Figures 1 and 2 show this variation for platinum [7, 8]. The rapid increase in both n and k with wavelength in the IR, typical of very good conductors, is responsible for the very high reflectivities common in Pt, Au, Cu, Al, and other metals.

Previous comparisons of methods for measuring n and k considered narrower spectral ranges and fewer methods than we do here. Most studies focused on measurements of reflectivity vs angle for obtaining n and k in the visible and UV. Humphreys–Owen [9] did the original work in this area but did not include methods that measured the relative phase shift on

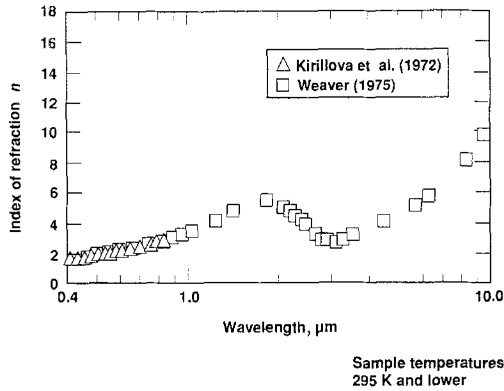

Fig. 1. Real part n of the complex index of refraction of platinum. See text for full reference citations.

reflection. He considered values of n from roughly 0.75 to 5 and of k from roughly 0 to 3. This region of n, k space includes very little of the IR for good conductors. In several papers [10–12], Hunter treated the visible to vacuum UV (VUV) range but ignored ellipsometric approaches because of the dearth of adequate polarizers for the VUV. Hunter considered a subset of the methods covered by Humphreys–Owen and used a different plotting format.

Several other studies have treated this subject more briefly. Miller et al. [13] considered only measurements of reflectance vs angle over a wavelength range similar to that of Humphreys–Owen. Their conclusions were

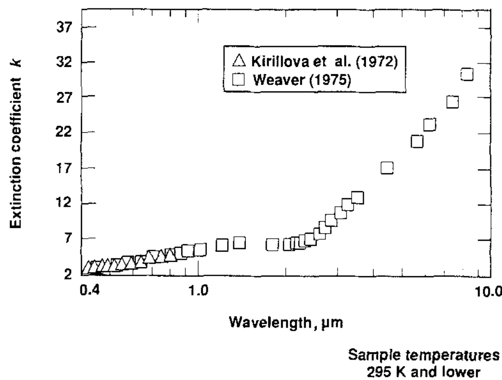

Fig. 2. Imaginary part k of the complex index of refraction of platinum. See text for full reference citations.

similar to those of Humphreys–Owen. Field and Murphy [14] and Graves and Lenham [15] also considered aspects of these methods.

A thorough consideration of all the potential methods over the full spectral range of interest can help in choosing the best experimental method. Methods with a high sensitivity (meaning that small uncertainties in measured values lead to large uncertainties in n and k) should be avoided over the entire spectral range of interest. The use of a single technique for the entire range is preferable for simplicity, reliability, and low cost.

The sensitivity study reported here is more complete in its consideration of methods and spectral range than previous work but is still limited in that it does not include many practical aspects of each method. Measurements of actual values (e.g., of reflectivity or emissivity, as in methods A and B below) are in general more difficult than measurements of ratios of values (as in methods C and D below). The difficulty of working with a light beam at angles extremely close to grazing incidence is another practical aspect. At grazing incidence the elliptical "footprint" of an incident beam changes very rapidly with angle. Measuring the average angle of incidence of a beam very near grazing is also difficult. These aspects are not assessed here.

2. BACKGROUND

The Fresnel equations describe the specular reflectance of an isotropic material for light in vacuum incident at angle θ:[3]

$$\begin{aligned} \rho_{\lambda,p} &\equiv r^2_{\lambda,p}(\lambda,\theta) = \frac{a^2+b^2-2a\sin\theta\tan\theta+\sin^2\theta\tan^2\theta}{a^2+b^2+2a\sin\theta\tan\theta+\sin^2\theta\tan^2\theta}\, r^2_{\lambda,s} \\ \rho_{\lambda,s} &\equiv r^2_{\lambda,s}(\lambda,\theta) = \frac{a^2+b^2-2a\cos\theta+\cos^2\theta}{a^2+b^2+2a\cos\theta+\cos^2\theta} \end{aligned} \tag{1}$$

where

$$2a^2 = [(n^2-k^2-\sin^2\theta)^2+4n^2k^2]^{1/2}+(n^2-k^2-\sin^2\theta)$$

and

$$2b^2 = [(n^2-k^2-\sin^2\theta)^2+4n^2k^2]^{1/2}-(n^2-k^2\sin^2\theta)$$

The amplitude reflection coefficient is r and the intensity reflection coefficient is ρ. Reflection methods for determining n and k are based on

[3] Definitions of symbols are given under Nomenclature.

these equations. Most often, polarized-reflection measurements are made at two or more angles of incidence, and then an n, k pair that best fits the measurements is computed. Emission measurements are also, in effect, based on the Fresnel equations. With optically thick samples, emissivity (the fraction of maximum possible emitted radiation from a body due to its temperature) and reflectivity can be simply related if the restrictions of Kirchhoff's law [16] apply:

$$\varepsilon'_\lambda(\lambda, \theta, T) = 1 - \rho'_\lambda(\lambda, \theta, T) \tag{2}$$

Emission methods, like reflection methods, can use the Fresnel equations, ratios of the two polarized components, or special features of the equations such as the minimum in the parallel component of reflectivity [9].

Ellipsometric methods use both the amplitude attenuation of a wave on reflection and the relative phase shift between the two components of polarization on reflection. These quantities are again functions of the angle of incidence and of n and k:

$$\begin{aligned} \varepsilon/\varepsilon_0 &= (n^2 - k^2) = \sin^2\theta \left\{1 + \tan^2\theta \left[\frac{\cos^2 2\psi - \sin^2 2\psi \sin^2 \Delta}{(1 + \sin 2\psi \cos \Delta)^2}\right]\right\} \\ \varepsilon'/\varepsilon_0 &= 2nk = 2\sin^2\theta \tan^2\theta \left[\frac{\cos 2\psi \sin^2 2\psi \sin \Delta}{(1 + \sin 2\psi \cos \Delta)^2}\right] \end{aligned} \tag{3}$$

with

$$\begin{aligned} \tan\psi &= |r_p|/|r_s| \\ \theta &= \text{angle of incidence} \\ \Delta &= \text{relative phase shift on reflection} \end{aligned} \tag{4}$$

3. METHODS EXAMINED

We considered six measurement methods:

(A) measurements of unpolarized reflectivity at two angles of incidence, which are fitted to the Fresnel equations to deduce n and k [17];

(B) measurements of emissivity at two angles of emission, which are fitted to the Fresnel equation to deduce n and k;

(C) measurements of the ratio of perpendicular to parallel polarized reflectivity, which are fitted to the Fresnel equations to deduce n and k [18];

(D) measurements of the ratio of perpendicular to parallel polarized emissivity at two angles of incidence, which are fitted to the Fresnel equations to deduce n and k [19];

(E) the method of Beattie and Conn [20, 21], in which a single angle of incidence and a rotating polarizer are used to deduce amplitude attenuation and relative phase shift on reflection and, thence, n and k; and

(F) the method of Miller [22], in which two azimuths (polarizer rotational positions) yielding equal intensity are determined by rotating both a polarizer and an analyzer. The angles for equal intensity are then used to deduce the phase shift and amplitude attenuation on reflection and, thence, n and k.

In method A, the average of the two polarized reflectivities is measured at two angles of incidence and an n, k pair is computed that best fits the measurements. In method B, emissivity is measured at two angles of emision and a similar fit is made to $1-(\rho'_{\lambda,s}+\rho'_{\lambda,p})/2$, since on a directional spectral basis, Kirchhoff's law [16] holds without restriction. In method C, the ratio of the two Fresnel equations is used. The measured values for this ratio at two angles of incidence are then fitted to the ratio $\rho'_{\lambda,p}/\rho'_{\lambda,s}$ to find the best n, k pair. In method D, the ratio $(1-\rho'_{\lambda,p})/(1-\rho'_{\lambda,s})$ is formed so that a similar procedure can yield the best n, k pair.

In method E, the polarizer or the analyzer is rotated between four positions. The phase shift and amplitude attenuation on reflection are related to four measured quantities I_1 to I_4 by the equations

$$\hat{\rho}(\theta) = \tan\psi = \sqrt{I_2/I_1}$$
$$\cos\Delta = \left[\frac{1}{2}\left(\hat{\rho}+\frac{1}{\hat{\rho}}\right)\right]\left(\frac{I_3-I_4}{I_3+I_4}\right) \tag{5}$$

The four measurements correspond to the four pairs of polarizer and analyzer positions first used by Beattie and Conn [20, 21].

In method F, the azimuthal angles for equal intensity are each used to determine ρ and Δ, and these are used to give n and k as in method E. The relations involving the polarizer azimuths Q_1 and Q_2 for equal intensity were given by Miller [22]:

$$\hat{\rho}^2 = \tan\ |Q_2| \tan |Q_1|$$
$$\cos(\Delta) = \frac{1}{2\hat{\rho}}(\tan|Q_1| - \tan|Q_2|) \tag{6}$$

4. SENSITIVITY CRITERIA

Two factors are involved in comparing the merits of the measurement schemes with regard to the accuracy of the inferred n, k values. These are (1) the spacing of contours of constant values of the measured variables and (2) the angles at which these contours intersect. If the two measured quantities are represented by x_1 and x_2 and their estimated uncertainties by δx_1 and δx_2, then the uncertainties δn and δk in the inferred n, k values are given by

$$\begin{aligned} \delta n &= \left(\frac{\partial n}{\partial x_1}\right)\delta x_1 + \left(\frac{\partial n}{\partial x_2}\right)\delta x_2 \\ \delta k &= \left(\frac{\partial k}{\partial x_1}\right)\delta x_1 + \left(\frac{\partial k}{\partial x_2}\right)\delta x_2 \end{aligned} \tag{7}$$

The quantities $\partial n/\partial x_1$, $\partial n/\partial x_2$, $\partial k/\partial x_1$, and $\partial k/\partial x_2$, which may be referred to collectively as sensitivity factors, can be found by differentiating the relevant equations (e.g., the Fresnel equations for methods A to D). The sensitivity factors are themselves functions of n and k and of the angle or angles of incidence at which the measurements are made. In practice, because of the complexity of the Fresnel relations, it is difficult to obtain analytic expressions for the sensitivity factors, and a more practical procedure (adopted here) is to plot contours of constant x_1, x_2 in the n, k plane. Moving from one point to another along any contour of constant x_1 can involve changes in n, k, or both. In the limit of very small displacement, one obtains $(\partial x_2/\partial n)x_1$ and $(\partial x_2/\partial k)x_1$ or, alternatively, their inverses, $\partial n/\partial x_2$ and $\partial k/\partial x_2$.

There are, of course, a great number of methods not included among the six considered here. The principal reasons for rejecting most of the others were (1) difficulty in applying them over the full spectral range of interest and (2) an obvious difficulty in applying them to hot metal samples, which must be in ultrahigh vacuum to maintain high surface purity.

Variations on methods A to D that use measurements at more than two angles are also not considered here, even though many have been reported [23]. The use of statistics and error-minimizing procedures makes these methods superior to, but fundamentally the same as, their simpler counterparts. Similar variations employing overdetermined systems could also be envisioned for methods E and F, so that our conclusions concerning the relative sensitivities of the methods would be essentially unchanged.

Variations on method D can provide improved accuracy and precision. For example, the polarizers can be synchronously rotated and

Fourier detection used [5, 6]. A full discussion of such methods is given by Hauge [24].

The results presented in the next section treat each method over the full parameter space discussed above $[0.3 < (n, k) < 40]$. In each case, contours of constant values of the measured quantities are plotted in the n, k plane. Since n and k are the desired quantities in all the methods, this puts all six methods on the same footing. Earlier works have most often plotted contours of constant values of the components of the complex refractive index, so that different methods are not as easily compared.

Several aspects of the contours are common to all the methods and are important in understanding and interpreting the results. The angle of intersection of the contours is critical when contours for the two measured quantities for a given method are plotted on the same grid. If the contours are nearly orthogonal, the two measured quantities are largely independent of one another. This is desirable since it implies that each measurement determines one of the two optical constants independent of the other measurement. If the contours are nearly parallel (with angles of intersection $\leqslant 20°$, say), the quantities are strongly dependent. In the limit that the contours intersect at very low angles or are parallel, the two quantities differ only by a multiplicative constant. In this case, the method cannot yield both n and k, because only a single independent quantity is in effect being measured. For example, if both slopes are zero, any uncertainty in either measured variable translates into an uncertainty in n but not in k (for n the abscissa); hence k cannot be determined. Similarly, for both contours vertical, n cannot be determined. For parallel slopes at other angles, a single quantity is determined and one cannot accurately obtain both n and k. Thus, as the contours in a given plot become less orthogonal, the method becomes less able to obtain both n and k. All six of the methods described here exhibit less orthogonal contours at the longer IR wavelengths, but the ellipsometric methods are always superior to the others in this respect.

Another important feature of the sensitivity plots is contour spacing. For a constant numerical difference between plotted contours, there is greater sensitivity in regions where contours are more closely spaced. That is, for a given uncertainty in the value of a measured quantity, the regions of closely spaced contours possess better sensitivity because the corresponding uncertainty in the components of the complex refractive index is less. (In the plotting scheme of Humphreys-Owen, the reverse is true.) When the uncertainty in both the measured quantities is considered at some position on a sensitivity plot, a corresponding uncertainty in both index components can be determined. In some studies [10–12], these uncertainties were themselves plotted to compare methods. However, as

Humphreys–Owen noted, sensitivity variations for a given method can be deduced fairly simply given an uncerstanding to these contour-spacing and orthogonality arguments.

5. RESULTS

5.1. Method A: Measurements of Unpolarized Reflectivity at Two Angles of Incidence

Figures 3 and 4 give contour plots for this method. The contours are lines of constant reflectivity for angles of incidence of 20 and 75°. Other pairs of angles would give somewhat different results, but greatly improved results can only be obtained by making one angle closer to grazing than 75°. Figures 3 and 4 (and all subsequent figures) cover a specified n, k range and therefore an approximate wavelength range. For many clean metals the range $0.3 < (n, k) < 4$ covers the visible and part of the UV.

In the lower-left corner of Fig. 3 (small n and k), the contour lines are largely orthogonal, indicating that the two measured quantities are largely independent of one another and that two unknows can be accurately determined from them. However, in the upper-right corner (n and k approaching 4) the contour lines are far less orthogonal, indicating decreased capability for determining two unknowns. Both sets of contours

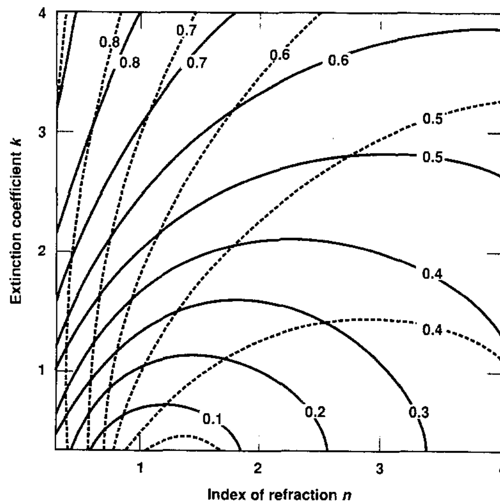

Fig. 3. Lines of constant $\rho(\theta_1)$ and $\rho(\theta_2)$ for $0.3 < (n, k) < 4$. Solid lines, $\theta_1 = 20°$; dashed lines, $\theta_2 = 75°$.

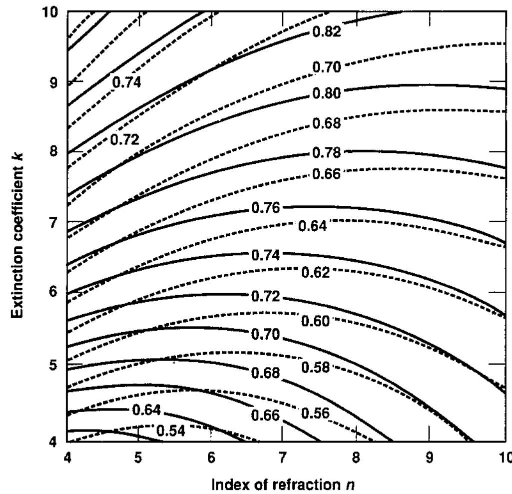

Fig. 4. Lines of constant $\rho(\theta_1)$ and $\rho(\theta_2)$ for $4<(n,k)<10$. Solid lines, $\theta_1=20°$; dashed lines, $\theta_2=75°$.

are approaching a horizontal slope in this region of the figure. Thus, method A has a low and decreasing capacity for the determination of n as n and k become larger than values typical of the visible region for metals.

Figure 4 presents results for method A for $4<(n,k)<10$, corresponding to wavelengths of $\sim$1–5 μm. The contour lines are even closer to parallel than in Fig. 3, particularly for the highest values of n and k. Clearly, method A is inadequate for complex index determination in the IR. Historically, this method has been valuable in the UV, where the polarizing optics required for other methods are not available.

5.2. Method B: Measurement of Emissivity at Two Angles of Emission

Methods A and B are similar in principle [because method A works with $\rho'_\lambda(\theta)$ and method B works with $1-\rho'_\lambda(\theta)=\varepsilon'_\lambda(\theta)$], but they differ in practice. Emission methods at angles approaching 90° are much more practical than their reflection counterparts, i.e., grazing-incidence reflection experiments. For this reason, angles of emission of 70 and 85° were chosen for the contour plots in Figs. 5 and 6. The n, k ranges used in Figs. 5 and 6 are the same as in Figs. 3 and 4 to make comparison easier.

In Fig. 5 the contours exhibit adequate spacing and orthogonality over most of the plot. The lower left-hand corner (small n and k) in Fig. 5 contains a region of nearly parallel contours, but this corresponds to the blue end of the visible range, or the UV.

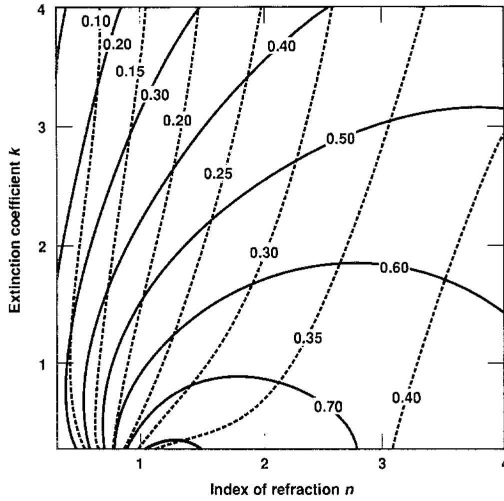

Fig. 5. Lines of constant $\varepsilon(\theta_1)$ and $\varepsilon(\theta_2)$ for $0.3 < (n, k) < 4$. Solid lines, $\theta_1 = 70°$; dashed lines, $\theta_2 = 85°$.

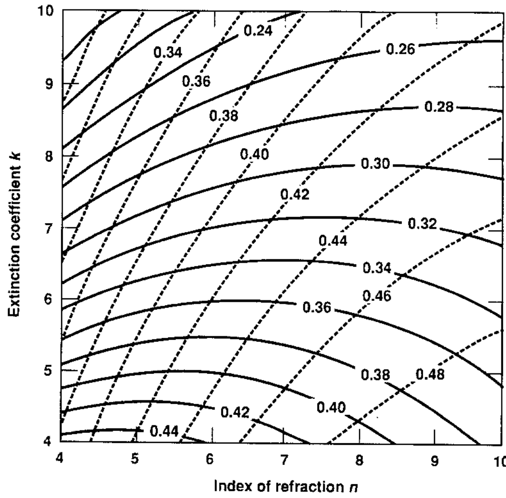

Fig. 6. Lines of constant $\varepsilon(\theta_1)$ and $\varepsilon(\theta_2)$ for $4 < (n, k) < 10$. Solid lines, $\theta_1 = 70°$; dashed lines, $\theta_2 = 85°$.

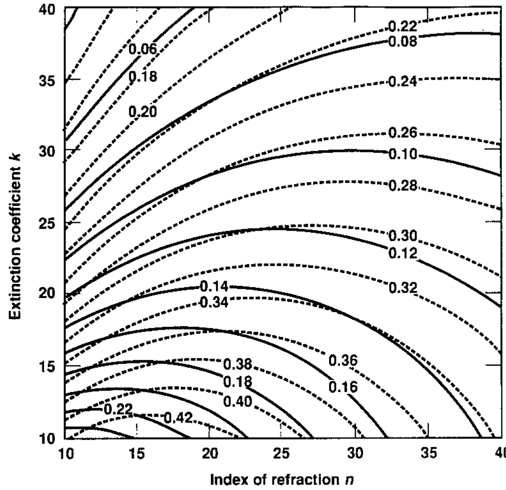

Fig. 7. Lines of constant $\varepsilon(\theta_1)$ and $\varepsilon(\theta_2)$ for $10 < (n, k) < 40$. Solid lines, $\theta_1 = 70°$; dashed lines, $\theta_2 = 85°$.

In Fig. 6, both sets of contours indicate good sensitivity over the full range plotted. The results in Figs. 5 and 6 indicate that method B could be adequate through the visible and some way into the IR. Figure 7 shows contours similar to those in Figs. 5 and 6 but for the range $10 < (n, k) < 40$. Once again, the contours are nearly parallel, indicating a poor capacity for discerning two unknowns from the two measurements. Thus, method B is adequate over a wider spectral range than method A and is probably much simpler experimentally (no input optics are required). However, good results cannot be expected from method B in the 3- to 10-μm spectral range.

5.3. Method C: Measurements of the Ratio of Perpendicular to Parallel Polarized Reflectivities

Measurements of the ratio of polarized reflectivities are effective over a wider spectral range and can be experimentally simpler than absolute reflectivity measurements such as those described above. As in method A, two angles of incidence are selected for the measurement positions and the results are fitted to the ratio of the two Fresnel equations. Figure 8 shows what corresponds to a visible spectral range $[0.3 < (n, k) < 4]$. Again, other pairs of measurement angles could have been selected, but this pair is representative. The contour lines are nearly orthogonal in the entire range shown. Since method C does not require an absolute reflectivity measure-

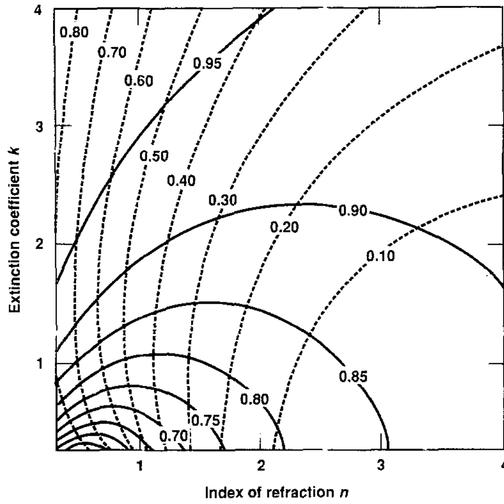

Fig. 8. Lines of constant $\rho_p(\theta_1)/\rho_s(\theta_1)$ and $\rho_p(\theta_2)/\rho_s(\theta_2)$ for $0.3 < (n, k) < 4$. Solid lines, $\theta_1 = 20°$; dashed lines, $\theta_2 = 75°$.

ment, it is clearly to be preferred to method A in the visible. For liquid samples, method C is particularly suited because the meniscus of a liquid makes absolute measurements very difficult (variation in the meniscus can significantly change optical throughput).

Figure 9 shows contours for an IR spectral range $[4 < (n, k) < 10]$.

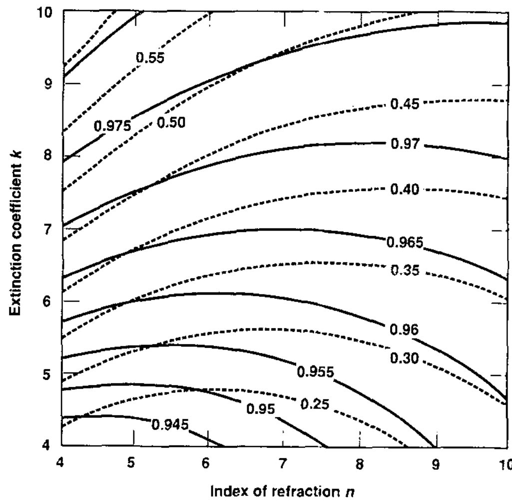

Fig. 9. Lines of constant $\rho_p(\theta_1)/\rho_s(\theta_1)$ and $\rho_p(\theta_2)/\rho_s(\theta_2)$ for $4 < (n, k) < 10$. Solid lines, $\theta_1 = 20°$; dashed lines, $\theta_2 = 75°$.

The contours are more nearly orthogonal in this range for method C than for method A (Fig. 4), but the difference is not substantial. For larger n, k, this method gives nearly parallel contours and is therefore inadequate. In summary, method C is preferred over method A but is ineffective in the long-wavelength extreme ($\lambda > 5\ \mu m$ or $n, k > \sim 20$).

5.4. Method D: Measurement of the Ratio of the Perpendicular to the Parallel Polarized Emissivity at Two Angles of Incidence

This method is the emissivity counterpart to method C and again possesses significant experimental advantages over methods A and B. No input optical system is required, absolute measurements are not required, and grazing emission is preferable to grazing reflection. Method D has been used extensively. Tingwaldt et al. [25] were particularly successful in applying this approach. (Data from 14 incidence angles between 0 and 70° were fitted to the Fresnel equations.) Their results for tungsten agreed well with the direct emissivity measurements of DeVos [26], Larrabee [27], and Latyev et al. [28], using the hole-in-tube technique.

Figures 10 and 11 show the results for this method using incidence angles of 20 and 75°. For the lower values of n, k shown in Fig. 10, the contours are well spaced but not adequately orthogonal. This is not a severe handicap for this method, since only for very hot samples is there substantial emission in the wavelength range corresponding to these n, k

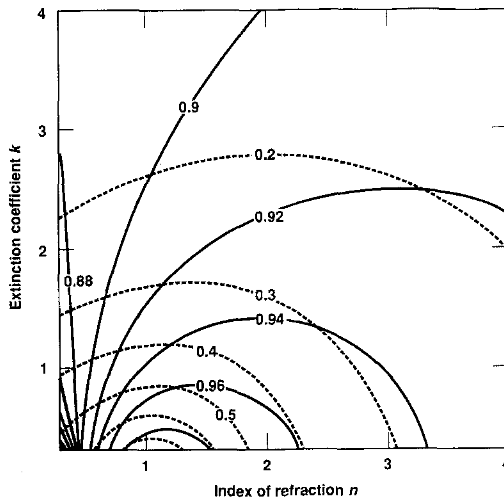

Fig. 10. Lines of constant $\varepsilon_s(\theta_1)/\varepsilon_p(\theta_1)$ and $\varepsilon_s(\theta_2)/\varepsilon_p(\theta_2)$ for $0.3 < (n, k) < 4$. Solid lines, $\theta_1 = 20°$; dashed lines, $\theta_2 = 75°$.

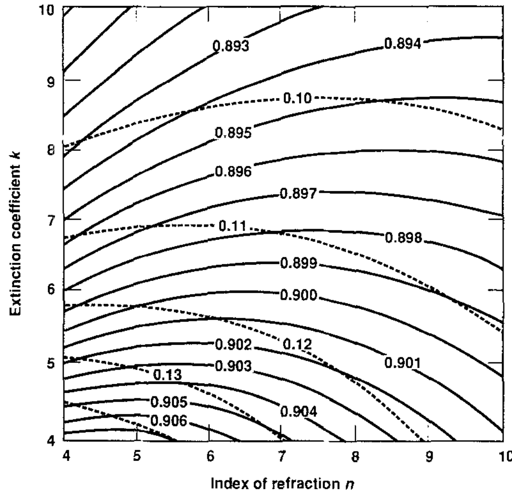

Fig. 11. Lines of constant $\varepsilon_s(\theta_1)/\varepsilon_p(\theta_1)$ and $\varepsilon_s(\theta_2)/\varepsilon_p(\theta_2)$ for $4 < (n, k) < 10$. Solid lines, $\theta_1 = 20°$; dashed lines, $\theta_2 = 75°$.

values. For intermediate n, k values typical of the visible and near IR, Fig. 10 exhibits acceptable orthogonality.

In Fig. 11 the contours are much more nearly parallel, just as in the 4–10 range for n and k for method C (Fig. 9). For $10 < (n, k) < 40$, Fig. 12 shows the contours to be even more nearly parallel. The upper-left corner

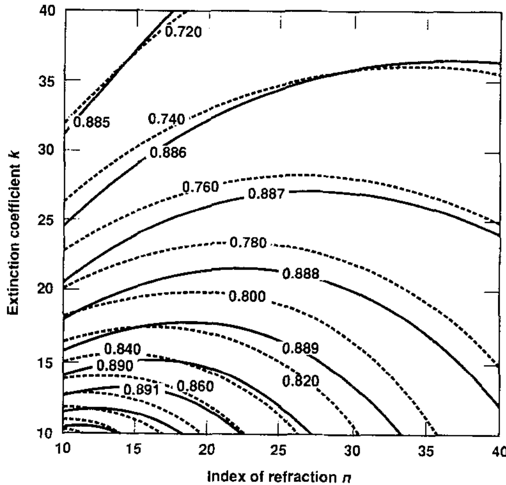

Fig. 12. Lines of constant $\varepsilon_s(\theta_1)/\varepsilon_p(\theta_1)$ and $\varepsilon_s(\theta_2)/\varepsilon_p(\theta_2)$ for $10 < (n, k) < 40$. Solid lines, $\theta_1 = 20°$; dashed lines, $\theta_2 = 75°$.

in Fig. 12 contains n, k values appropriate for many metals in the 8- to 10-μm range. The spacing between contours in this range shows that very small errors in the measured variables will result in substantial changes in both n and k. For example, the contours corresponding to $\theta_1 = 20°$ are 0.885 and 0.886 in this corner of the figure. For a change of 0.001 in the ratio of polarized emissivities measured for this value of θ_1, the appropriate contour for determining n and k changes from the 0.885 line to the 0.886 line. Moving from one to the other of these two contours represents a large change in both n and k. The combination of the separation of these two contours in n, k space and the nearly parallel contours for the two measurement angles makes it clear that this method is not viable at 8 to 10 μm.

When normal spectral emissivity is of interest rather than n and k themselves, the sensitivity criteria discussed here are also useful. In spectral ranges where spectral emissivity measurements have a relatively poor sensitivity for obtaining n and k, there must be a good sensitivity for obtaining a normal spectral emissivity from n and k. In other words, a region where small changes in spectral emissivity produce large changes in n and k is a region where small changes in n and k produce very small changes in spectral emissivity. This trend was confirmed experimentally by Tingwaldt et al. [25].

5.5. Method E: The Method of Beattie and Conn

Figures 13–15 show contour plots for method E for an angle of incidence of 75° and a polarizer azimuth of 45°. It was too cumbersome to plot contours of constant values of the measured quantities I_1 through I_4; instead we used the reduced quantities M_1 and M_2, where

$$M_1 = \sqrt{\frac{I_2}{I_1}}; \qquad M_2 = \frac{I_3 - I_4}{I_3 + I_4} \tag{8}$$

The orthogonality of the contours of M_1 and M_2 in Fig. 13 indicate the potential effectiveness of method E in the visible. Although both sets of contours are curved, they remain very nearly orthogonal over the entire range plotted.

Figure 14 shows the n, k range $4 < (n, k) < 10$. Both the contour spacing and the orthogonality indicate that the method will be effective. Figure 15 shows the n, k range $10 < (n, k) < 40$. The contours still intersect at nearly right angles.

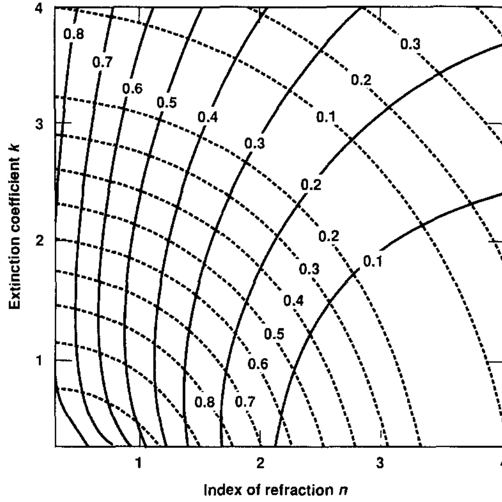

Fig. 13. Lines of constant M_1 and M_2 for $0.3 < (n, k) < 4$. Solid lines, M_1; dashed lines, M_2. Angle of incidence, 75°.

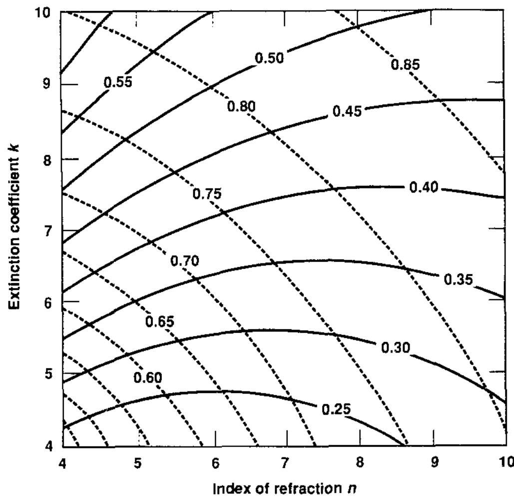

Fig. 14. Lines of constant M_1 and M_2 for $4 < (n, k) < 10$. Solid lines, M_1; dashed lines, M_2. Angle of incidence, 75°.

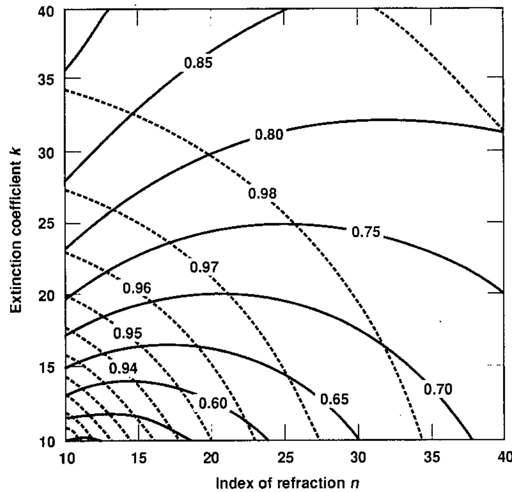

Fig. 15. Lines of constant M_1 and M_2 for $10 < (n, k) < 40$. Solid lines, M_1; dashed lines, M_2. Angle of incidence, 75°.

5.6. Method F: The Method of Miller

This is a variation on method E. The values of $\hat{\rho}$ and Δ are determined from measurements of the two angles of the analyzer for which the intensities are equal for two given settings of the polarizer. Finding the positions of equal intensity is not as convenient and is considerably slower than recording four intensities at regular polarizer positions, as in method E.

Figures 16–19 show contour plots for method F. In Figs. 16–18, the angle of incidence and polarizer azimuth are again 75 and 45°, respectively. In Fig. 19 the angle of incidence was changed to 84°. The contours in all three plots are lines of constant values of polarizer azimuth Q_1 and Q_2 for equal intensities. In Fig. 16 the contour lines are nearly orthogonal over the entire plot $[0.3 < (n, k) < 4]$. Methods E and F are very similar in this range for the same (75°) angle of incidence. In Fig. 17, for $4 < (n, k) < 10$, the contours are also adequately orthogonal, and the sensitivity is comparable to that in method E. In Fig. 18 $[10 < (n, k) < 40]$, however, the lines of constant measured position are decidedly more parallel than in Fig. 15, the corresponding case for method E. This indicates that method F has a lower sensitivity than method E in the long-wavelength extreme for a 75° angle of incidence. Other practical factors may override the indications from these figures, but from a fundamental standpoint, the method of Beattie and Conn appears superior (method F does not require a linear detector, however).

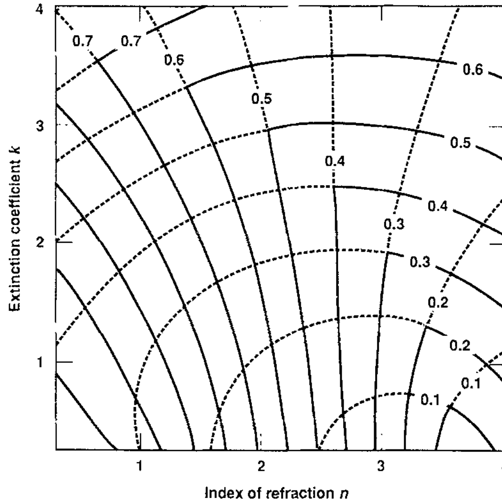

Fig. 16. Lines of constant Q_1 and Q_2 for $0.3 < (n, k) < 4$. Solid lines, Q_1; dashed lines, Q_2. Angle of incidence, 75°.

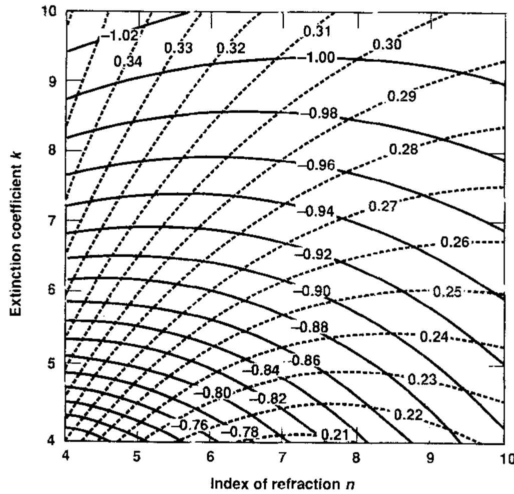

Fig. 17. Lines of constant Q_1 and Q_2 for $4 < (n, k) < 10$. Solid lines, Q_1; dashed lines, Q_2. Angle of incidence, 75°.

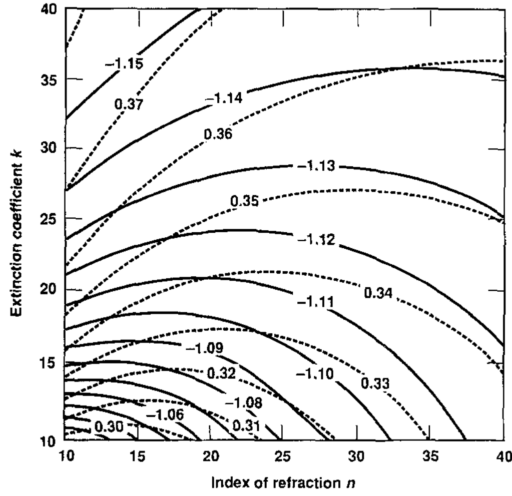

Fig. 18. Lines of constant Q_1 and Q_2 for $10<(n, k)<40$. Solid lines, Q_1; dashed lines, Q_2. Angle of incidence, 75°.

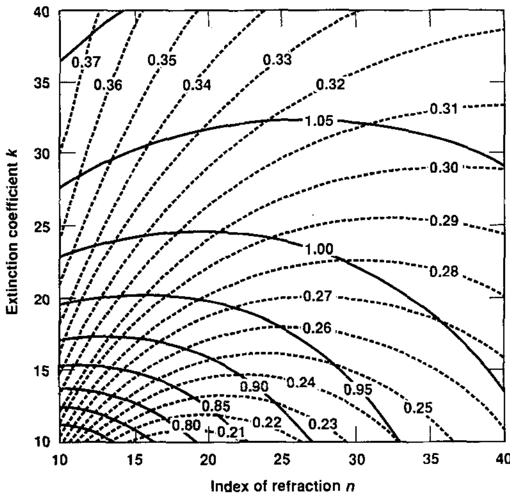

Fig. 19. Lines of constant Q_1 and Q_2 for $10<(n, k)<40$. Solid lines, Q_1; dashed lines, Q_2. Angle of incidence, 84°.

Figure 19 gives results for method F for $10 < (n, k) < 40$ with the angle of incidence increased to 84° (the angle used by Miller [22] in some of her experiments). The orthogonality of the contours shown in Fig. 19 is comparable to that of method E with a 75° angle of incidence (Fig. 15). Substantial advantages in fundamental sensitivity would require working even closer to grazing incidence than 84°.

5.7. Results with the Method of Beattie and Conn

The sensitivity and effectiveness calculations given above led us to select the method of Beattie and Conn for measurements of the optical constants of liquid uranium (melting point 1406 K) [29]. Measurement system performance was good to 5 μm and adequate to 8.5 μm. Beyond ~5 μm, experimental difficulties (such as chromatic effects with transmissive optics, decreasing detector sensitivity, and decreasing radiation source strength) were severe.

The method was also used to determine the optical and radiative properties of high-temperature solid tungsten, perhaps the best studied metal. Comparisons were very favorable over the entire spectral range of interest [30]. The somewhat lower precision in the results of the present study (for both components of the refractive index and the normal spectral emissivity computed from them) was an expected consequence of the compromises necessary to allow measurements on liquid metals.

The optical constants of liquid aluminum have also been determined [31]. Good agreement with prior works [22,32] was obtained.

6. CONCLUSIONS

The sensitivity of available methods for the measurement of optical constants of metals in the wavelength range 0.4 to 10 μm varies greatly. Reflection methods are well suited to the visible, but rapidly become ineffective in the IR. Measurements using ratios of polarized emission or reflection are effective in the near-IR and are simpler to implement, but performance decreases rapidly with increasing wavelength wavelength. For applications where visible and IR measurements to 10 μm are required, spectroscopic ellipsometry is attractrive. The method of Beattie and Conn is preferred at such long wavelengths and is experimentally more convenient than the variant method developed by Miller [22]. For applications where the optical constants are required from 0.4 to 10 μm, such as for heat transfer calculations, the method of Beattie and Conn is preferred.

ACKNOWLEDGMENT

This work was performed under the auspices of the U.S. Department of Energy by Lawrence Livermore National Laboratory under Contract W-7405-Eng-48.

NOMENCLATURE

a, b	Terms in the Fresnel equations
I	Intensity
I_1, I_2, I_3, I_4	Measured values in ellipsometric technique
k	Extinction coefficient
M_1, M_2	Reduced values in an ellipsometric technique
n	Index of refraction
N	Complex index of refraction
Q_1, Q_2	Measured values in an ellipsometric technique
r	Amplitude reflection coefficient
x, y	Rectilinear coordinates
x_1, x_2	Dummy variables

Greek Letters

δ	Phase angle
ε	Emissivity
θ	Angle
λ	Wavelength
ρ	Intensity reflection coefficient
$\hat{\rho}$	Ratio of amplitude reflection coefficients
ψ	Angle used in ellipsometry
Δ	Relative phase shift on reflection
ε	Real part of complex dielectric function
ε'	Imaginary part of complex dielectric function
ε_0	Permittivity of free space

Subscripts

p	Parallel component
s	Perpendicular component
x, y	Cartesian coordinate directions
λ	Wavelength

Superscripts

$'$	Directional quantity, except when used with ε, where it denotes the real part

REFERENCES

1. D. W. Lynch and W. R. Hunter, in *Handbook of Optical Constants of Solids, Part II, Subpart 1*, E. D. Palik, ed. (Academic Press, New York, 1985), pp. 275–367.
2. E. N. Shestakov, L. N. Latyev, and V. Ya. Chekhovskoi, *High Temp.* **16**:140 (1978).
3. S. Mattei, P. Masclet, and P. Herve, *Infrared Phys.* **29**:991 (1989).
4. E. T. Arakawa, T. Inagaki, and M. W. Williams, *Surface Sci.* **96**:248 (1980).
5. S. Krishnan et al., *High Temp. Sci.* **29**:17 (1990).
6. S. Krishnan et al., *High Temp. Sci.* **30**:137 (1991).
7. M. M. Kirillova, L. V. Nomerovannaya, and M. M. Noskov, *Fiz. Metal. Metalloved.* **34**:60 (1972).
8. J. H., Weaver, *Phys. Rev. B* **11**:1416 (1975).
9. S. P. F. Humphreys-Owen, *Proc. Phys. Soc.* **77**:949 (1961).
10. W. R. Hunter, in *Handbook of Optical Constants of Solids*, E. D. Palik, ed. (Academic Press, New York, 1985), pp. 69–88.
11. W. R. Hunter, *J. Opt. Soc. Am.* **55**:1197 (1965).
12. W. R. Hunter, *Appl. Opt.* **21**:2103 (1982).
13. F. R. Miller, A. J. Taylor, and L. S. Julien, *J. Phys. D* **3**:1957 (1970).
14. G. R. Field and E. Murphy, *Appl. Opt.* **10**:1402 (1971).
15. R. H. W. Graves and A. P. Lenham, *J. Opt. Soc. Am.* **58**:884 (1968).
16. R. Siegel and J. R. Howell, in *Thermal Radiation Heat Transfer*, 2nd ed. (McGraw–Hill, New York, 1981), pp. 57–60.
17. I. Simon, *J. Opt. Soc. Am.* **41**:336 (1951).
18. D. G. Avery, *Proc. Phys. Soc. B* **65**:425 (1952).
19. A. Kinbara, *J. Phys. Soc. Jap.* **13**:966 (1958).
20. J. R. Beattie, *Phil. Mag.* **46**:235 (1955).
21. J. R. Beattie and G. K. T. Conn, *Phil. Mag.* **46**:222 (1955).
22. J. C. Miller, *Phil. Mag.* **20**:1115 (1969).
23. W. S. Martin, E. M. Duchane, and H. H. Blau, *J. Opt. Soc. Am.* **55**:1623 (1965).
24. S. Hauge, *Surf. Sci.* **96**:108 (1980).
25. C. Tingwaldt, U. Schley, J. Verch, and S. Takata, *Optik* **22**:48 (1965).
26. J. C. DeVos, *Physica* **XX**:690 (1954).
27. R. D. Larrabee, *J. Opt. Soc. Am.* **49**:619 (1959).
28. L. N. Latyev, V. Ya. Chekhovskoi, and E. N. Shestakov, *High Temp. High Press.* **2**:175 (1970).
29. M. A. Havstad, W. McLean II, and S. A. Self, 28th ASME/AiChE National Heat Transfer Conference, San Diego, CA, (1992), Publ. No. HTD-Vol. 203, pp. 9–17.
30. M. A. Havstad, W. McLean II, and S. A. Self, *Rev. Sci. Instrum.*, in press.
31. M. A. Havstad, Ph.D. dissertation (Stanford University, Palo Alto, CA, 1991); Lawrence Livermore National Laboratory, Livermore, CA, UCRL-LR-107524 (1991).
32. N. R. Comins, *Phil. Mag.* **25**:817 (1972).